Journal of Biomedical Science **12:** 197–207, 2005.
DOI 10.1007/s11373-004-8166-8

The role of nitric oxide in the spatial heterogeneity of basal microvascular blood flow in the rat diaphragm

Cheng-Hung Lee, Han-Yu Chang*, Chang-Wen Chen & Tzuen-Ren Hsiue
Department of Internal Medicine, College of Medicine, National Cheng Kung University, Tainan 704, Taiwan, ROC

Received 17 October 2004; accepted in revised form 4 November 2004

Key words: L-arginine, laser-Doppler scanning, N^G-monomethyl-L-arginine, N^ω-nitro-L-arginine, respiratory muscle, spatial heterogeneity

Summary

The effects of N^ω-nitro-L-arginine (L-NOARG) and N^G-monomethyl-L-arginine (L-NMMA) on the spatial distribution of diaphragmatic microvascular blood flow were assessed in anesthetized, mechanically ventilated rats. Microvascular blood flow was measured after different periods at either a fixed site (Q_{stat}) or 25 different sites (Q_{scan}) using computer-aided laser-Doppler flowmetry (LDF) scanning. The value of Q_{stat} was unaffected after 15–20 min superfusion with any one of the following agents: L-NOARG (0.1 mM), L-NMMA (0.1 mM), L-arg (10 mM). The cumulative frequency histogram of the Q_{scan} value in the control group displayed a non-Gaussian distribution that was not significantly affected after 15 min superfusion with the vehicle of L-NOARG. Superfusion with either L-NMMA or L-NOARG at 0.1 mM for 15 min displaced the histogram of cumulative frequency to the left, with the median value of blood flow decreasing by 10 to 20%. However, skewness and kurtosis of the distribution of basal Q_{scan} were unaffected after superfusion of either of the L-arg analogues. Pretreatment with L-arg (10 mM), followed by co-administration of L-arg (10 mM) with L-NOARG (0.1 mM) only partially prevented L-NOARG from exerting this inhibitory effect on the distribution of basal Q_{scan}, while pretreatment with L-arg in the same manner could prevent L-NMMA from exerting its inhibitory effect. There was a weak but significant linear relationship between the magnitude of basal Q_{scan} and normalized changes in basal Q_{scan} after superfusion of either of the L-arg analogues. In conclusion, a basal NO activity is present in the diaphragmatic microvascular bed of rats. LDF scanning rather may yield more vivid information about the extent of overall tissue perfusion than conventional LDF whenever basal NO activity is involved. Moreover, the parallel flow profiles after NO synthase blockade suggest that the spatial inhomogeneity of basal diaphragmatic microvascular blood flow is not dependent on basal NO formation.

Introduction

Diaphragmatic blood flow is a crucial factor in determining the function of the diaphragm because decreased contractive force of the diaphragm in low blood flow states can lead to respiratory failure [1, 2]. It has been shown that diaphragmatic vascular tone in the isolated canine diaphragm under basal conditions is partially regulated by NO [3, 4]. In diaphragmatic microcirculation, which ultimately determines perfusion adequacy, N^ω-nitro-L-arginine (L-NOARG) has been shown to cause a significant reduction in A_2 arteriolar diameters in a dose-dependent manner [5]. On the contrary, our previous studies using laser-Doppler flowmetry (LDF) showed that baseline NO activity in the diaphragmatic

*To whom correspondence should be addressed. Fax: +886-6-2087310; E-mail: hychang@mail.ncku.edu.tw

microvascular bed of resting rats is quite low, and that neither N^{ω}-nitro-L-arginine methyl ester (L-NAME) nor L-NOARG can affect basal microcirculatory blood flow [6]. Since there is a wide spatial heterogeneity of diaphragmatic microvascular blood flow [8], the issue is raised that vasomotor responses recorded over a single site in the diaphragm may not be representative of the entire area of the vascular bed being studied.

Observations in several preparations including coronary vascular beds and striated muscles have suggested that variation in the importance of the NO pathway among arterioles of different diameters is a common phenomenon [8–11]. Similarly, longitudinal gradients of NO-mediated dilatation of arterioles have been identified in isolated canine diaphragms, as shown by an ability of L-NOARG to induce vasoconstriction, which is linearly related to the basal diameters of arterioles [12]. To clarify the relationship between basal NO activity and spatial inhomogeneity of diaphragmatic microcirculation, study of flow information from multiple sites is necessary. Collection of this information can be accomplished with LDF, and multi-spots scanning can be done with either an integrating probe [13], or a laser-Doppler perfusion imager [14]. However, the former technique requires a luxurious space to accommodate the big probe head (diameter = 6 mm), while the latter method demands meticulous examination of off-line microscopic images to exclude flow values originating from major visible vessels. To avoid these problems, the present study used computer-aided LDF scanning to measure blood flow over multiple locations in the diaphragm. Information concerning the distribution of tissue microvascular blood flow was obtained by analysis of the central location and spread of frequency histograms.

The aim of this study was to assess the role of NO in the spatial heterogeneity of diaphragmatic microcirculation under basal conditions. Rat diaphragms were prepared to allow recording of information about the spatial heterogeneity of microcirculation by LDF scanning. Both L-NOARG and N^{G}-monomethyl-L-arginine (L-NMMA) were used as specific pharmacological tools to block NO synthase, and the ability of L-arginine (L-arg) to prevent these L-arg analogues from exerting their inhibitory effects on basal NO formation was also assessed.

Methods

Animal preparation

Male Sprague–Dawley rats (weight 300–350 g) were housed at the Laboratory Animal Center of the College of Medicine at National Cheng Kung University. All animals were maintained on Purina rat chow and tap water *ad libitum*. The animals were fasted overnight the day before the experiment.

The animals were initially anesthetized with intraperitoneal sodium pentobarbital (30 mg/kg body wt) followed by intravenous 50% w/v urethane (1.2–1.5 g/kg body wt) and placed in a supine position on a rodent operating table. After tracheostomy, muscle relaxant (gallamine triethiodide; 60 mg/kg body wt) was administered, and the rats were artificially ventilated at tidal volumes between 6–7 ml/kg body wt and a rate of 70–80 breaths/min. Supplemental O_2 was given via the inspiratory port. Mean systemic blood pressure (MAP) was measured with a polyethylene catheter (PE-50) inserted via the right carotid artery and connected to a pressure transducer. A cardiotachometer triggered by the pulse pressure signal was used to monitor the heart rate. Normal saline (3–5 ml/h/100 g body wt) was infused into the left external jugular vein throughout the experiment via a peristaltic pump. Rectal temperature was continuously monitored with a thermistor and maintained at 36–38 °C by a heating lamp and a temperature-regulated bed.

Diaphragm preparation

The techniques used for diaphragm preparation have been described in detail elsewhere [7]. Briefly, thoracotomy was performed in the right fifth and sixth intercostal spaces, and a 1 cm long segment of the right sixth rib was removed. The diaphragm was separated from the lungs and the mediastinal tissues. An ovoid-shaped stainless steel plate coated with white glossy acrylic was slipped behind the diaphragm to hold the left hemidiaphragm flat.

Midline and transverse abdominal incisions were made and the ligament between the liver and the central tendon was severed. With the animal in the Trendelenburg position, the upper abdominal wall was folded back and retracted. Abdominal

viscera were immobilized by wrapping them with a plastic cast. Superfusion of the abdominal side of the left hemi-diaphragm at a flow rate of 5 ml/min was begun immediately after exposure, using bicarbonate-buffered Ringer's solution equilibrated with 5% CO_2 and 95% N_2. The temperature of the superfusing fluid was maintained at 37 °C. A side port connected to a syringe pump was set up for administration of drugs. The infusion rate was set at 1% of the rate of the superfusing fluid to standardize the final concentration of test agents.

Laser-Doppler flowmetry

A commercially available LDF monitor (Laserflo BPM^2, Vasamedics, St. Paul, MN, USA) equipped with a 0.8-mm needle probe (model P 443-3) was used to measure microvascular flow rates. The probe was held in a stepping motor-driven micromanipulator (Eppendorf micromanipulator 5171, Hamburg, Germany) with a resolution of 0.16 μm per microstep. Probe movements could be controlled manually either by joystick or computer. The control program was written in the Visual Basic programming language (Microsoft Inc., Redmond, WA, USA). The probe was placed perpendicular to the surface of the diaphragm, with the probe tip just touching the water film of the suffusate on the surface of the diaphragm. A starting site without visible large vessels on the left costal diaphragm was chosen by visualization with a long-working-distance stereoscopic zoom microscope (SMZ-10A, Nikon, Tokyo, Japan). The signal output from the LDF was a DC voltage (Q_{LDF}, updated 8 times/s). The time constant was set at 1 s.

Drugs

Urethane, gallamine triethiodide, dextran 70, adenosine, L-arginine hydrochloride, and L-NOARG were obtained from Sigma Chemical (St. Louis, MO, USA). L-NMMA was obtained from Research Biochemical Int. (Natick, MA, USA). All of the compounds except urethane and L-NOARG were prepared fresh daily in saline and stored on ice during the experiments. Urethane was prepared in saline at a 50% w/v concentration. L-NOARG was dissolved in a saline solution containing dimethyl sulfoxide (DMSO, final concentration 0.1%) and NaOH (final concentration 0.9 mN) to obtain a final concentration of 10 mM.

Experimental protocols

Experiments were initiated after a 30- to 45-min stabilization period. Arterial blood gas and hematocrit were determined. The animals used in this study met the following criteria during the stabilization period: (1) MAP > 80 mmHg, (2) pH 7.35–7.45, PO_2 > 100 mmHg, (3) Hct > 40%, (4) greater than twofold increases in the Q_{LDF} compared with baseline values after topical application of adenosine at 0.1 mM, and (5) no obvious hemorrhage in the muscle tissue under investigation. Seven series of experiments were performed. After the stabilization period, the first cycle of laser-Doppler scanning was started on the surface of the left hemi-diaphragm. The scanning probe was translocated to 25 different sites by a micromanipulator under computer control. The Q_{LDF} obtained during the scanning period was defined as the Q_{scan}. These sites were all situated on a line at 100-μm intervals centripetally from the starting point to the central tendon of the diaphragm. The path of the probe could easily be selected to be free of large vessels with the aid of the microscope. The scan speed was set at 100 μm/s to reduce motion artifacts. An average reading time of 20 s was required to provide a stable signal that was independent of vasomotion for each point of measurement. Therefore, one cycle of scanning took approximately 9 min. After the first cycle of scanning, the probe was moved back to the starting position, and was fixed in this position for the next 15–20 min, while the diaphragm was exposed to test agents. The Q_{LDF} obtained during this period was thus defined as the Q_{stat}. In series 1, nine rats received topical saline at 1% of the flow rate of the suffusion fluid for 15 min (the time-control group). In 10 rats in series 2 and 8 rats in series 3, either L-NOARG or L-NMMA at 0.1 mM was applied to the preparation for 15 min by continuous suffusion, respectively. In 10 rats in series 4 and 8 rats in series 5, after pretreatment with L-arg at 10 mM for 5 min, L-arg (10 mM) was co-administered with either L-NOARG (0.1 mM) or L-NMMA (0.1 mM), respectively, for another 15 min. In 6 rats in series 6, L-arg (10 mM) was topically

administered to the preparation for 20 min. Finally, in eight rats in series 6, the vehicle of L-NOARG was suffused for 15 min. After these procedures, the second cycle of multi-spot scanning was performed at identical coordinates. At the end of the experiments, all the animals were sacrificed with an intravenous injection of saturated potassium chloride. The last cycle of scanning was performed to obtain the postmortem signals at 25 sites, which were considered as individual biological zero and subtracted from the corresponding Q_{scan} values. Since baseline physiological values and the Q_{scan} obtained in animals of series 1 (time-control) and series 7 (vehicle-control) showed no significant difference, the data were pooled for analysis.

Data acquisition and statistical analysis

MAP and Q_{LDF} data were fed into the chart recorder (Gould RS 3200 polygraphy) for continuous recording. The output of pressure signals, heart rate, and the analog output from the LDF was directed into a multichannel analog interphase unit, where the signal was sampled at 10 Hz with a 12-bit analog-to-digital converter (AT codas, Dataq Instrument, Akron, OH, USA) and stored in a personal computer. Recording periods complicated by artefacts were excluded before data analysis. The average Q_{LDF} during a recording time of 20 s was defined as one measurement.

Data was tested for Gaussian distribution using a Kolmogorov–Smirov one sample test. Systemic physiological variables and the Q_{stat} were expressed as means ± SE, and the Q_{scan} as median (range). The value of Q_{LDF} recorded at the starting site of the scanning was defined as baseline microvascular blood flow. Differences in baseline values of systemic and microcirculatory physiological variables among groups were analysed for statistical significance using analysis of variance, followed by Student's t test with Bonferroni correction if necessary. Student's t test for paired data was used to analyse the difference between the values of Q_{stat} obtained before and after superfusion with test agents. The Q_{scan} distribution profile was presented as a frequency histogram, and the Kolmogorov–Smirnov two-sample test was used to examine differences in the distribution between histograms. Additionally, the median value, skewness and kurtosis of histograms before and after NO synthase blockade were compared using Wilcoxon signed-ranks test. The relationship between baseline Q_{LDF} and percent changes of baseline Q_{LDF} in animals of the L-NOARG group and the L-NMMA group was examined by Spearman rank correlation coefficient analysis. A value of $p < 0.05$ was considered statistically significant.

Results

Systemic and microcirculatory variables

The results described below are from experiments carried out on 59 rats that met the inclusion criteria for MAP, arterial blood gases and Hct: MAP was 98 ± 1 mmHg, heart rate was 416 ± 4 per min, arterial pH was 7.41 ± 0.01, arterial PO_2 was 131.9 ± 2.3 mmHg, arterial PCO_2 was 34.2 ± 0.3 mmHg, and Hct was 45 ± 1%. The resting Q_{LDF} was 268 ± 14 mV. There were no significant differences in baseline MAP, heart rate, or Q_{LDF} among animals of the six experimental groups, as shown in Table 1 ($p = 0.104$, 0.26, and 0.932, respectively).

Responses of basal Q_{stat}

Topical application of L-NOARG or L-NMMA both at 0.1 mM for 15 min did not affect basal Q_{stat} ($p = 0.445$, and 0.123, respectively). Pretreatment with L-arg 10 mM for 5 min, followed by co-administration of L-arg 10 mM and either L-NOARG or L-NMMA 0.1 mM for another 15 min, did not affect basal Q_{stat} ($p = 0.646$ and 0.889, respectively). Moreover, superfusion of L-arg 10 mM did not have a significant effect on basal Q_{stat} ($p = 0.893$) (Table 2). Since all drugs were topically applied to the surface of the diaphragm, there was no significant change in MAP following the administration of any drug (data not shown).

Responses of basal Q_{scan}

Figure 1 shows a continuous tracing of Q_{LDF} recorded for over 45 min in a single animal in the control group. The tracing representatively illustrates the value of Q_{scan} recorded at 25 different sites at each of the two scanning cycles, and Q_{stat} recorded over a fixed site before and after suffusion of the vehicle for 15 min.

Table 1. Baseline mean systemic arterial blood pressure (MAP), heart rate (HR) and diaphragmatic microvascular blood flow recorded by laser-Doppler flowmetry (Q_{LDF}) in animals of six experimental groups.

	MAP (mmHg)	HR (min^{-1})	Q_{LDF} (mV)
Control (n = 17)	99 ± 4	415 ± 8	274 ± 38
L-NOARG (n = 10)	101 ± 3	427 ± 8	268 ± 34
L-NMMA (n = 8)	105 ± 3	426 ± 8	242 ± 38
L-arg + L-NOARG (n = 10)	94 ± 3	420 ± 8	292 ± 34
L-arg + L-NMMA (n = 8)	98 ± 3	423 ± 8	255 ± 38
L-arg (n = 6)	91 ± 4	399 ± 10	231 ± 44

Values are mean ± SE. L-NOARG, N^{ω}-nitro-L-arginine (0.1 mM); L-NMMA, N^{G}-monomethyl-L-arginine (0.1 mM); L-arg + L-NOARG, L-arginine (10 mM) co-administered with N^{ω}-nitro-L-arginine (0.1 mM); L-arg + L-NMMA, L-arginine (10 mM) co-administered with N^{G}-monomethyl-L-arginine (0.1 mM); L-arg, L-arginine (10 mM); n, the number of animals in each experimental group.

Table 2. Changes of diaphragmatic microvascular blood flow (Q_{stat}, mV) recorded by laser-Doppler flowmetry at a fixed site after 15–20 min suffusion with test agents.

	Before	After
Control (n = 17)	241 ± 32	298 ± 40
L-NOARG (n = 10)	274 ± 40	249 ± 28
L-NMMA (n = 8)	221 ± 31	213 ± 33
L-arg + L-NOARG (n = 10)	291 ± 35	320 ± 45
L-arg + L-NMMA (n = 8)	257 ± 23	255 ± 18
L-arg (n = 6)	216 ± 37	230 ± 34

Abbreviations as shown in Table 1.

A normalized frequency histogram of a total of 425 baseline Q_{scan} data values in the control group is shown in Figure 2a. The histogram exhibits an obvious non-Gaussian distribution ($p < 0.001$, skewness = 1.894, and kurtosis = 4.139), with a median flow at 261 mV (51–1202 mV). Figure 2b illustrates that in the control group there was no significant difference between the two cumulative frequency histograms of Q_{scan}, obtained before and after suffusion of the saline or vehicle, with the median flow changing from 261 mV (51–1202 mV) to 274 mV (75–1218 mV) ($p = 0.545$).

Figure 3a illustrates that topical application of L-NOARG at 0.1 mM for 15 min displaced the histogram of cumulative relative frequency to the left ($p < 0.001$), and the median decrease of blood flow was roughly 20%, changing from 239 mV (113–881 mV) to 189 mV (66–501 mV). However, the skewness of histograms did not change significantly before and after the administration of L-NOARG (0.87 ± 0.16 vs. 0.77 ± 0.20, $p = 0.508$), and kurtosis of histograms also remained unaffected (0.75 ± 0.45 vs. 0.76 ± 0.47, $p = 0.721$). Figure 3b reveals that pretreatment with L-arg (10 mM), followed by co-administration

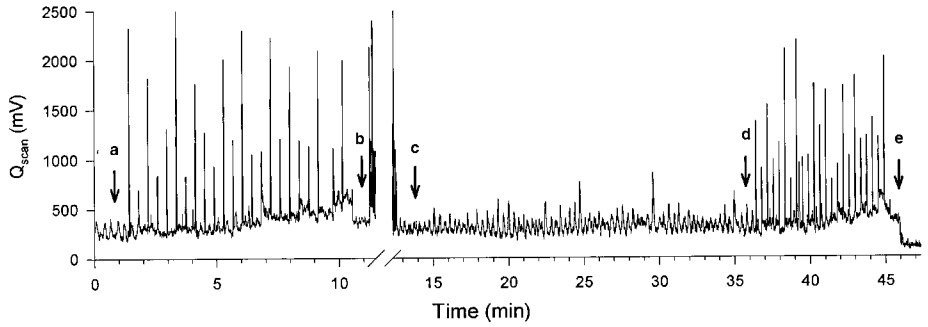

Figure 1. A typical tracing of Q_{scan}, as measured by laser-Doppler flowmetry, illustrating the spatial heterogeneity of the diaphragmatic microvascular blood flow in a vehicle-treated rat over a 45-min period. Arrows indicate the timing of events [(a) the first cycle of scanning over 25 different sites; (b) moving the probe back to the origin; (c) the start of recording over a fixed site; (d) the second cycle of scanning over 25 different sites]. The spikes with an amplitude greater than 750 mV are caused by movement of the probe.

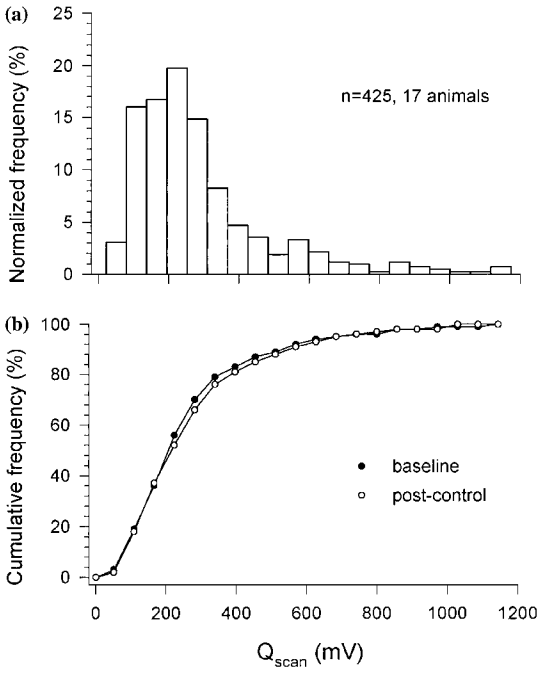

Figure 2. A normalized frequency histogram (panel a) obtained by pooling Q_{scan} data from laser-Doppler scanning of the surface of the left hemi-diaphragm in 17 rats in the control group. Twenty-five sites in 100-μm intervals were measured in each rat. The histogram reveals a non-Gaussian distribution ($p < 0.001$, skewness = 1.894, and kurtosis = 4.139), with a median flow at 261 mV. Histograms of cumulative relative frequency (panel b) showed no significant change in the distribution of Q_{LDF} in the control group (•, baseline; ○, post time- and vehicle-control, $n = 425$ in each distribution), with the median flow changing from 261 to 274 mV ($p = 0.545$).

of L-arg (10 mM) with L-NOARG (0.1 mM) only partially prevented L-NOARG from exerting this inhibitory effect on the distribution of basal blood flow ($p < 0.001$). The median blood flow still decreased by 10%, from 259 mV (102–664 mV) to 231 mV (89–752 mV).

Figure 4a demonstrates that suffusion of L-NMMA at 0.1 mM for 15 min shifted the curve of cumulative relative frequency to the left ($p < 0.001$), and there was a 12% reduction in the median blood flow from 269 mV (42–942 mV) to 239 mV (11–528 mV). Nevertheless, there was no significant difference in either skewness (0.52 ± 0.45 vs. 0.33 ± 0.40, $p = 0.09$), or kurtosis of histograms (1.58 ± 1.22 vs. 1.22 ± 0.84, $p = 0.327$) before and after the administration of L-NMMA. Pretreatment with L-arg 10 mM, followed by co-administration of L-arg (10 mM) with L-NMMA (0.1 mM) completely restored the distribution profile of basal blood flow ($p = 0.987$) (Figure 4b). The change in the median blood flow, from 253 mV (53–1366 mV) to 238 mV (55–1211 mV), was not significant.

Analysis of pooled Q_{scan} data from both the L-NOARG group and the L-NMMA group revealed a significant linear relationship between the magnitude of basal Q_{scan} and normalized changes of basal Q_{scan} after superfusion with either L-NOARG or L-NMMA 0.1 mM for 15 min ($r = -0.29$, $p < 0.001$) (Figure 5).

The distribution of basal blood flow profiles was not significantly affected by topical administration of L-arg alone at 0.1 mM for 20 min ($p = 0.361$), and the median blood flow before and after suffusion of L-arg was 230 mV (76–834 mV) and 215 mV (58–667 mV), respectively ($p = 0.361$) (Figure 6).

Discussion

The results of this study show that: (1) there was a wide spatial heterogeneity of basal Q_{LDF} in rat

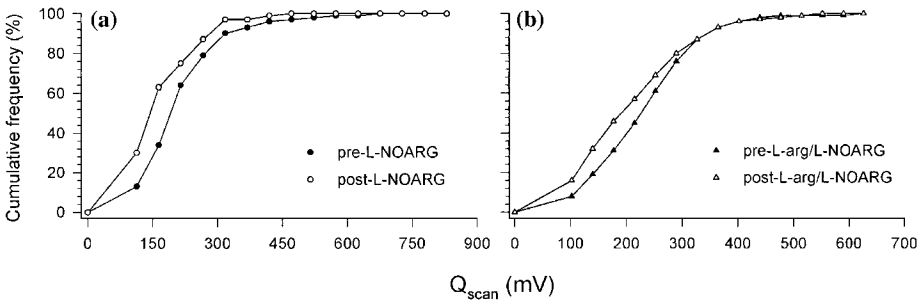

Figure 3. Cumulative relative frequency histograms of recorded Q_{scan} before (•) and after (○) superfusion with N^{ω}-nitro-L-arginine (L-NOARG, 0.1 mM) (panel a, $n = 250$ in each distribution, values from 10 animals), and before (▲) and after (△) superfusion of L-arginine (L-arg, 10 mM) coadministered with L-NOARG (0.1 mM) (panel b, $n = 250$ in each distribution, values from 10 animals).

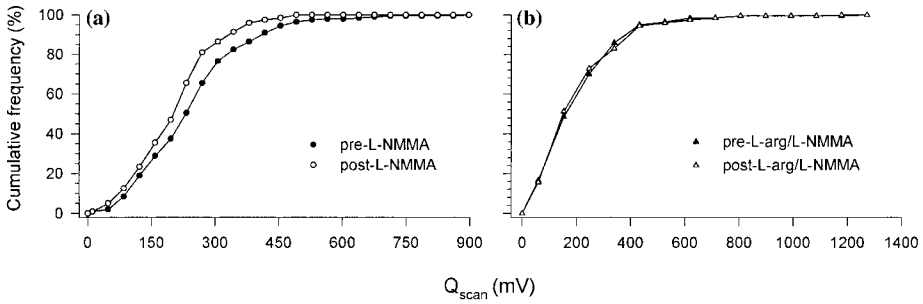

Figure 4. Distributions of recorded Q_{scan}, presented as cumulative relative frequency histograms, before (•) and after (○) superfusion with N^G-monomethyl-L-arginine (L-NMMA, 0.1 mM) (panel a, $n = 200$ in each distribution, values from eight animals), and before (▲) and after (△) superfusion of L-arginine (L-arg, 10 mM) coadministered with L-NMMA (0.1 mM) (panel b, $n = 200$ in each distribution, values from eight animals).

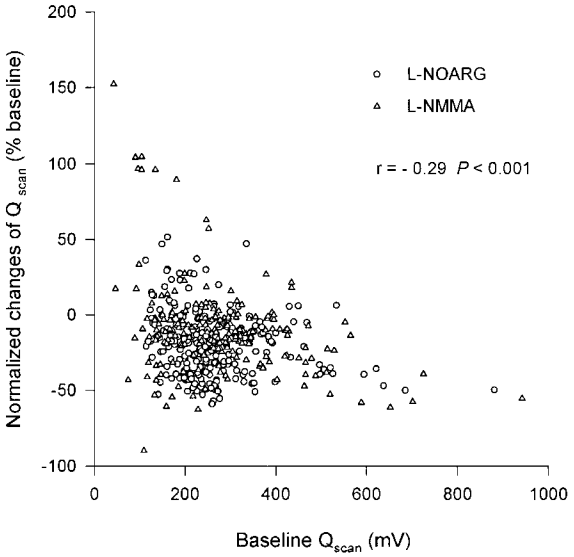

Figure 5. Relationship between normalized changes of Q_{scan} and baseline Q_{scan}, after suffusion of either L-NOARG (0.1 mM, ○) or L-NMMA (0.1 mM, △). Note the weak but significant linear correlation coefficient ($r = -0.29$, $p < 0.001$).

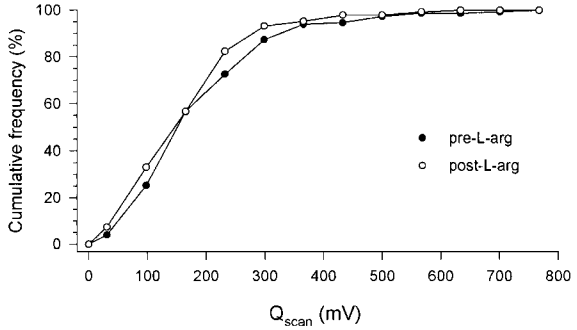

Figure 6. Distributions of recorded Q_{scan}, presented as cumulative relative frequency histograms, before (•) and after (○) superfusion of L-arginine (L-arg, 10 mM) ($n = 150$ in each distribution, values from six animals).

diaphragms; (2) the value of Q_{stat} recorded over one fixed site did not reflect the fact that NO was involved in the maintenance of basal diaphragmatic blood flow; (3) the frequency histograms of multi-spot Q_{scan} data revealed that basal NO played a role in resting diaphragmatic microcirculation through its effects on a reduction of the median value of Q_{scan} rather than a decrease of flow heterogeneity; (4) vasoconstrictive effects induced by either L-NOARG or L-NMMA were somewhat related to the level of basal blood flow, while the former was a more potent inhibitor of NO synthase, and less likely to be reversed by L-arg than the latter.

Currently, available LDF technology limits investigations to small regionally heterogeneous volumes of diaphragmatic microcirculation [7]. This was reflected in the wide spread of resting Q_{scan} in our study. Previous studies have reported a similar wide variation in individual basal Q_{LDF}, with variations up to 3.7-, 4-, and 10-fold in rat brain cortex, canine stomach, and nasal mucosa, respectively [15–17]. Likely explanations for the spatial variation of Q_{scan} may be related to the variability in the average velocities of moving red blood cells, local hematocrit, or the number of capillaries containing flowing blood.

In the current study, the acquisition of Q_{scan} data required sequential translocation of the probe to 25 different sites over a 9-min period. Frequency histograms of Q_{scan}, therefore, included both spatial inhomogeneity over the 25 sites and temporal changes during this period, i.e., temporal variations of the Q_{scan}. Since the Q_{stat} data obtained from experimental animals were stable over a

period of 15–20 min, most of the variations of Q_{scan} were probably caused by spatial heterogeneity of Q_{scan} itself.

Spatial variations in diaphragmatic microcirculation made the quantitative assessment of tissue blood flow difficult. However, after normalization of Q_{LDF} to 100% at baseline, the LDF at a fixed probe position seems a very promising technique for measuring the acute effects of pathophysiological and pharmacological stimuli [6, 18, 19]. Similarly, local pharmacological studies using LDF have also been performed in rat kidney, human skin, and human nasal mucosa [16, 20–22].

In the current study, diaphragmatic microcirculation under basal conditions, as reflected by changes of the Q_{stat} recorded from a single site, was not affected by local superfusion of either L-NOARG or L-NMMA. This result is consistent with our previously reported findings [6]. The data suggested that basal NO activity in the diaphragmatic microcirculation was quite low and that NO probably did not play a significant role in modulating resting Q_{LDF} in the anesthetized rats. In contrast, baseline diaphragmatic vascular resistance was shown to increase by 28% of control values after L-NOARG was directly infused into the phrenic artery in vascularized isolated canine diaphragms [4]. Moreover, intravital microscopy showed that topical applications of L-NOARG dose-dependently caused a significant reduction in A_2 arteriolar diameters ranging from 3 to 15.7% of control values in resting rat diaphragms [5]. One possible explanation for these contradictory results is that in the rat diaphragm preparation the LDF was used to measure a heterogenous microvascular bed, and the overall change in microvascular response is probably not predictable from the change of Q_{LDF} recorded at a single tissue site. Support for this explanation is provided by findings that the amplitude of a neurogenic vasomotor response can be affected by the magnitude of basal Q_{LDF} in cat lips [23], and that vasomotor responses to pharmacological stimuli vary in different size arterioles in the coronary microcirculation [24–26].

To clarify the relative contributions of basal NO activity and spatial inhomogeneity to the modulating resting Q_{LDF} of the diaphragmatic microcirculation, collection of flow information from multiple sites over a short interval will be necessary. In the present study, LDF scanning was used to measure blood flow over multiple locations in the diaphragm. By detecting changes in the median and range of histograms of cumulative relative frequency, LDF scanning can reveal information concerning the distribution of tissue microvascular blood flow. This scanning technique has been successfully applied to investigate a variety of pathophysiological conditions in the cerebral cortex [27–29].

Suffusion of both arginine analogues in the current study led to a significant reduction of the median blood flow recorded from multiple sites, suggesting that basal NO played a role in modulating resting diaphragmatic microcirculation. Moreover, our data showed that L-NOARG was a more potent inhibitor of NO synthase than L-NMMA, as the former produced a 20% reduction and the latter a 12% reduction of median Q_{LDF}. Consistent with our results, biochemical assays have shown that L-NOARG is 70-fold, and 200-fold more potent than L-NMMA in bovine aortic endothelial cells and rat brain tissues, respectively [30, 31].

In various vascular beds, L-arg can antagonize the effects of L-NOARG and L-NMMA [11, 32, 33]. Since L-NMMA can be transported into endothelial cells via saturable y^+ transporters, whereas L-NOARG cannot enter the cell via the y^+ system [34], the effects of L-NOARG are much more difficult to reverse than those of L-NMMA, requiring at least a 100-fold excess of the substrate both *in vivo* and *in vitro* [35]. In this study, pretreatment with L-arg in 100-fold excess followed by co-administration of L-arg with L-NMMA prevented the inhibitory effect by L-NMMA. On the contrary, similar administration of L-arg partially prevented L-NOARG from exerting its inhibitory effects on the distribution of basal Q_{LDF}. A similar phenomenon has also been reported in the regulation of renal blood flow in anesthetized rats, where a 3-fold excess of L-arg reversed L-NMMA-induced inhibition of baseline NO activity, while a 100-fold excess of L-arg only partially restored the inhibition of basal blood flow by L-NOARG [36]. However, L-arg in a 100-fold excess has also been reported to completely reverse L-NOARG-induced inhibitory effects on rat diaphragmatic arteriolar diameters, as observed by intravital microscope [12]. This discrepancy might have been due to the use of different anesthetics or differences in the methods used to measure microcirculation. Consistent with

our previously reported findings [6], L-arg alone at 10 mM did not affect basal microcirculatory blood flow or its distribution, suggesting that the availability of extracellular L-arg is not a rate-limiting factor in NO synthesis in this preparation.

There are two likely explanations for the observation that the Q_{stat} data failed to reveal the involvement of NO in our study. First, the method and technique used to prepare the diaphragm may have affected the Q_{stat} values. In the canine diaphragm, the effects of L-NOARG have been demonstrated to depend on the metabolic demand, with phrenic vascular resistance changing from an insignificant increase at rest to an 80% increase during periods of increased metabolic demand [37]. Accordingly, in the current study the use of a respirator coupled with muscle relaxants allowed complete rest of the diaphragm and avoided increased metabolic need. This metabolic status may have resulted in a low baseline NO activity in the region of diaphragmatic microcirculation sampled by the stationary probe.

A second explanation for the failure of Q_{stat} data to detect the involvement of NO may have been the spatial heterogeneity of basal NO activity in the diaphragmatic microvascular bed. This explanation seems to be supported by several observations. Studies in coronary circulation and skeletal muscle preparations have shown that variation in the importance of the NO pathway among arterioles of different diameters is an intrinsic characteristic [8–11, 38]. Moreover, in canine diaphragms the magnitude of vasoconstriction induced by L-NOARG has been demonstrated to be linearly related to the basal diameter of arterioles [12]. However, the present results showed that skewness and kurtosis of Q_{scan} data were not affected by either L-arg analogue, suggesting that the spatial heterogeneity of diaphragmatic microcirculation cannot be ascribed to a cross-sectional gradient in basal NO activity. Similar phenomena have been observed in both the canine hearts and cat hindlimbs, where blockade of local NO production had only minimal effects on the spatial heterogeneity of blood flow [39, 40].

Flow-dependent dilatation of arteriolar diameters has been demonstrated in rat spinotrapezius muscle preparations and isolated gracilis muscle arterioles [41, 42]. Furthermore, the wall shear stress imposed by streaming fluid has been shown to contribute to the formation of NO under basal conditions in rabbit coronary vascular beds [43]. However, our results revealed only a weak relationship between the magnitude of basal Q_{scan} and percent changes of Q_{scan} induced by L-arg analogues, suggesting that flow-mediated NO release may play a minor role in maintaining the spatial heterogeneity of basal diaphragmatic perfusion. Further study is needed to explore the possibility that local differences in diaphragmatic energy metabolism determine spatial diaphragmatic blood flow heterogeneity.

In summary, the results of this study indicate the presence of basal NO activity in diaphragmatic microvascular beds, and that the spatial inhomogeneity of microvascular blood flow is not dependent on NO. Therefore, whenever the involvement of basal NO formation is being considered, special caution should be taken in the interpretation of microcirculatory data acquired over a fixed site. Under these circumstances, laser-Doppler scanning may provide a more accurate assessment of tissue perfusion.

References

1. Hussain S.N.A. and Magder S., Respiratory muscle function in shock and infection. Semin. Respir. Med. 12: 287–297, 1991.
2. Viires N., Sillye M., Aubier M., Rassidakis A. and Roussos C., Effects of mechanic ventilation on respiratory muscle and regional blood flow distribution during cardiogenic shock. J. Clin. Invest. 72: 935–947, 1983.
3. Chang H.Y., Ward M.E. and Hussain S.N.A., Regulation of diaphragmatic oxygen uptake by endothelium-derived relaxing factor. Am. J. Physiol. 265: H123–H130, 1993.
4. Ward M.E. and Hussain S.N.A., Regulation of baseline vascular resistance in the canine diaphragm by nitric oxide. Br. J. Pharmacol. 112: 65–70, 1994.
5. Boczkowski J., Vicaut E., Danialou G. and Aubier M., Role of nitric oxide and prostaglandins in the regulation of diaphragmatic arteriolar tone in the rat. J. Appl. Physiol. 77: 590–596, 1994.
6. Chang H.Y., Chen C.W. and Hsiue T.R., Comparative effects of L-NOARG and L-NAME on basal blood flow and ACh-induced vasodilatation in rat diaphragmatic microcirculation. Br. J. Pharmacol. 120: 326–332, 1997.
7. Chang H.Y., Chen C.R. and Hussain S.N.A., Diaphragmatic microcirculation measured by laser-Doppler flowmetry. J. Appl. Physiol. 78: 1225–1233, 1995.
8. Ekelund U. and Mellander S., Role of endothelium-derived nitric oxide in the regulation of tonus in large-bore arterial resistance vessels, arterioles and veins in cat skeletal muscle. Acta Physiol. Scand. 140: 301–309, 1990.
9. Habazettl H., Vollmar B., Christ M., Baier H., Conzen P.F. and Peter K., Heterogeneous microvascular coronary

vasodilation by adenosine and nitroglycerin in dogs. J. Appl. Physiol. 76: 1951–1960, 1994.
10. Kuo L., Davis M.J. and Chilian W.M., Longitudinal gradients for endothelium-dependent and -independent vascular responses in the coronary microcirculation. Circulation 92: 518–525, 1995.
11. Persson M.G., Gustafsson L.E., Wiklund N.P., Hedqvist P. and Moncada S., Endogenous nitric oxide as a modulator of rabbit skeletal muscle microcirculation *in vivo*. Br. J. Pharmacol. 100: 463–466, 1990.
12. Ward M.E., Effect of inhibition of nitric oxide synthesis on the diaphragmatic microvascular response to hypoxia. J. Appl. Physiol. 81: 1633–1641, 1996.
13. Salerud E.G. and Nilsson G.E., Integrating probe for tissue laser-Doppler flowmeters. Med. Biol. Eng. Comput. 24: 415–419, 1986.
14. Lindéen M., Sirsjö A., Lindbom L., Nilsson G. and Gidlöf A., Laser-Doppler perfusion imaging of microvascular blood flow in rabbit tenuissimus muscle. Am. J. Physiol. 269: H1496–H1500, 1995.
15. Dirnagl U., Kaplan B., Jacewicz M. and Pulsinelli W., Continuous measurement of cerebral cortical blood flow by laser-Doppler flowmetry in a rat stroke model. J. Cereb. Blood Flow Metab. 9: 589–597, 1989.
16. Druce H.M., Bonner R.F., Patow C., Choo P., Summers R.J. and Kaliner M.A., Response of nasal blood flow to neurohormone as measured by laser-Doppler velocimeter. J. Appl. Physiol. 57: 1276–1283, 1984.
17. Gana T.J., Hunlewych R. and Koo J., Focal gastric mucosal blood flow by laser-Doppler and hydrogen gas clearance: a comparative study. J. Surg. Res. 43: 337–343, 1987.
18. Chang H.Y., The involvement of ATP-sensitive potassium channels in β_2-adrenoceptor agonist-induced vasodilatation on rat diaphragmatic microcirculation. Br. J. Pharmacol. 121: 1024–1030, 1997.
19. Chang H.Y., Chen C.W., Hsiue T.R. and Chen C.R., Role of K_{ATP} channels on modulating diaphragmatic microvascular flow during hemorrhagic hypotension. Am. J. Physiol. 272: H272–H278, 1997.
20. Bergström G., Rudenstam J., Taghipour K. and Göthberg G., Effect of nitric oxide and renal nerves on renomedullary hemodynamics in SHR and Wistar rats, studies with laser Doppler technique. Acta Physiol. Scand. 156: 27–36, 1996.
21. Stern M.D., Bowen P.D., Parma R., Osgood R.W., Bowman R.L. and Stein J.H., Measurement of renal cortical and medullary blood flow by laser-Doppler spectroscopy in the rat. Am. J. Physiol. 236: F80–F87, 1997.
22. Tur E., Maibach H.I. and Guy R.H., Spatial variability of vasodilatation in human forearm skin. Br. J. Dermatol. 113: 197–203, 1985.
23. Karita K. and Izumi H., Effect of baseline vascular tone on vasomotor responses in cat lip. J. Physiol. 482: 679–685, 1995.
24. Bund S.J., Oldham A.A. and Heagerty A.M., Influence of arterial diameter on vasomotor responses in the porcine coronary vasculature. Cardiovasc. Res. 28: 695–699, 1994.
25. Frame M.D.S. and Sarelius I.H., Regulation of capillary perfusion by small arterioles is spatially organized. Circ. Res. 73: 155–163, 1993.
26. Lamping K.G., Kanatsuka H., Eastham C.L., Chilian W.M. and Marcus M.L., Nonuniform vasomotor responses of the coronary microcirculation to serotonin and vasopressin. Circ. Res. 65: 343–351, 1989.
27. Heimann A., Kroppenstedt S., Ulrich P. and Kempski O.S., Cerebral blood flow autoregulation during hypobaric hypotension assessed by laser-Doppler scanning. J. Cereb. Blood Flow Metab. 14: 1100–1105, 1994.
28. Ungersböck K., Heimann A. and Kempski O.S., Cerebral blood flow alterations in a rat model of cerebral sinus thrombosis. Stroke 24: 563–570, 1993.
29. Ungersböck K., Tenckhoff D., Heimann A., Wagner W. and Kempski O.S., Transcranial Doppler and cortical microcirculation at increased intracranial pressure and during the Cushing response: an experimental study on rabbits. Neurosurgery 36: 147–157, 1995.
30. Ischii K., Chang B., Kerwin J.F. Jr., Huang Z.-J. and Murad F., N^{ω}-nitro-L-arginine: a potent inhibitor of endothelium-derived relaxing factor formation. Eur. J. Pharmacol. 176: 219–223, 1990.
31. Lambert L.E., Whitten J.P., Baron B.M., Cheng H.C., Doherty N.S. and McDonald I.A., Nitric oxide synthesis in the CNS, endothelium and macrophages differs in its sensitivity to inhibition by arginine analogues. Life Sci. 48: 69–75, 1991.
32. Gardiner S.M., Compton A.M., Bennett T., Palmer R.M. and Moncada S., Control of regional blood flow by endothelium-derived nitric oxide. Hypertension 15: 486–492, 1990.
33. Moore P.K., al-Swayeh O.A., Chong N.W.S., Evans R.A. and Gibson A., L-N^{G}-nitro arginine (L-NOARG), a novel, L-arginine-reversible inhibitor of endothelium-dependent vasodilatation *in vitro*. Br. J. Pharmacol. 99: 408–412, 1990.
34. Bogle R.G., Moncada S., Pearson J.D. and Mann G.E., Identification of inhibitors of nitric oxide synthase that do not interact with the endothelial cell L-arginine transporter. Br. J. Pharmacol. 105: 768–770, 1992.
35. Rees D.D., Palmer R.M., Schulz R., Hodson H.F. and Moncada S., Characterization of three inhibitors of endothelial nitric oxide synthase *in vitro* and *in vivo*. Br. J. Pharmacol. 101: 746–752, 1990.
36. Walder C.E., Thiemermann C. and Vane J.R., The involvement of endothelium-derived relaxing factor in the regulation of renal cortical blood flow in the rat. Br. J. Pharmacol. 102: 967–973, 1991.
37. Shen W., Lundborg M., Wang J., Stewart J.M., Wu W., Ochoa M. and Hintze T.H., Role of EDRF in the regulation of regional blood flow and vascular resistance at rest and during exercise in conscious dogs. J. Appl. Physiol. 77: 165–172, 1994.
38. Komaru T., Tanikawa T., Sugimura A., Kumagai T., Sato K., Kanatsuka H. and Shirato K., Mechanisms of coronary microvascular dilation induced by the activation of pertussis toxin-sensitive proteins are vessel-size dependent: heterogeneous involvement of nitric oxide pathway and ATP-sensitive K^{+} channels. Circ. Res. 80: 1–10, 1997.
39. Deussen A., Sonntag M., Flesche C.W. and Vogel R.M., Minimal effects of nitric oxide on spatial blood flow heterogeneity of the dog heart. Pflügers Arch. 433: 727–734, 1997.
40. Iversen P.O., Flateb T. and Nicolaysen G., Uneven perfusion within single cat muscles: nitric oxide and citrate synthase play no role. Respir. Physiol. 89: 329–339, 1992.

41. Friebel M., Klotz K.F., Ley K., Gaehtgens P. and Pries A.R., Flow-dependent regulation of arteriolar diameter in rat skeletal muscle *in situ*: role of endothelium-derived relaxing factor and prostanoids. J. Physiol. 483: 715–726, 1995.
42. Koller A., Sun D., Huang A. and Kaley G., Corelease of nitric oxide and prostaglandins mediates flow-dependent dilation of rat gracilis muscle arterioles. Am. J. Physiol. 267: H326–H332, 1994.
43. Lamontagne D., Pohl U. and Busse R., Mechanical deformation of vessel wall and shear stress determine the basal release of endothelium-derived relaxing factor in the intact rabbit coronary vascular bed. Circ. Res. 70: 123–130, 1992.